Frontiers of Information Technology & Electronic Engineering
www.jzus.zju.edu.cn; engineering.cae.cn; www.springerlink.com
ISSN 2095-9184 (print); ISSN 2095-9230 (online)
E-mail: jzus@zju.edu.cn

Improved three-vector based dead-beat model predictive direct power control strategy for grid-connected inverters*

Chen-wen CHENG, Heng NIAN†‡, Long-qi LI

College of Electrical Engineering, Zhejiang University, Hangzhou 310027, China

†E-mail: nianheng@zju.edu.cn

Received Dec. 29, 2016; Revision accepted Apr. 25, 2017; Crosschecked Nov. 26, 2018

Abstract: Since only one inverter voltage vector is applied during each duty cycle, traditional model predictive direct power control (MPDPC) for grid-connected inverters (GCIs) results in serious harmonics in current and power. Moreover, a high sampling frequency is needed to ensure satisfactory steady-state performance, which is contradictory to its long execution time due to the iterative prediction calculations. To solve these problems, a novel dead-beat MPDPC strategy is proposed, using two active inverter voltage vectors and one zero inverter voltage vector during each duty cycle. Adoption of three inverter vectors ensures a constant switching frequency. Thus, smooth steady-state performance of both current and power can be obtained. Unlike the traditional three-vector based MPDPC strategy, the proposed three vectors are selected based on the power errors rather than the sector where the grid voltage vector is located, which ensures that the duration times of the selected vectors are positive all the time. Iterative calculations of the cost function in traditional predictive control are also removed, which makes the proposed strategy easy to implement on digital signal processors (DSPs) for industrial applications. Results of experiments based on a 1 kW inverter setup validate the feasibility of the proposed three-vector based dead-beat MPDPC strategy.

Key words: Grid-connected inverter; Model predictive control; Direct power control; Three vectors; Constant switching frequency; Power errors

https://doi.org/10.1631/FITEE.1601874 **CLC number:** TM464

1 Introduction

The three-phase grid-connected inverter (GCI) usually works as the interface between renewable energy resources (RES) and the power grid due to its outstanding advantages, such as low current distortion, small dc-link capacitor value, controllable power factor, and bidirectional power flow (Rodriguez et al., 2005). With the fast development of RES, the GCI is playing a more and more important role in power systems (Zeng et al., 2016; Zhao et al., 2016; Chen et al., 2017).

Various control methods for GCIs have been proposed to obtain smooth steady-state performance of current and power, or fast dynamic responses. Among them, model predictive control (MPC) is emerging as an advanced control strategy and has received more and more attention. Different from the classical vector control (VC) strategy (Blasko and Kaura, 1997; Malinowiski, 2001) that treats the control system as linear and continuous, in MPC the nonlinear characteristic of power switches and discrete characteristics of digital control systems are used, and the future states of the GCI system are predicted based on the discrete model of the GCI and the present states. Nonlinear restrictions and requirements can be added to the control scheme to implement the selected control targets, such as low switching frequency (Vargas et al., 2007), controllable harmonic spectra (Cortes et al., 2008a), and low

‡ Corresponding author

* Project supported by the National Natural Science Foundation of China (No. 51622706) and the Fundamental Research Funds for the Central Universities, China (No. 2017XZZX002-17)

ORCID: Heng NIAN, http://orcid.org/0000-0003-4816-084X

common mode voltage (Dekka et al., 2017).

Model predictive direct power control (MPDPC) (Cortes et al., 2008b; Song et al., 2014) is one category of MPC strategies, and has the integrated advantages of both MPC and direct power control (DPC). In MPDPC, active power and reactive power are directly controlled without current loops. Thus, the control system is simple and compact. Based on the discrete model of the GCI, different values of active and reactive powers can be predicted with all available inverter vectors. The most suitable inverter vector that leads to the minimum value of the cost function is selected, which will be implemented during the next duty cycle.

However, the selection process is intuitive and varying switching frequency is inevitable (Zhang et al., 2013, 2014). As a result, a broad-band harmonic spectrum would be generated, which is difficult to suppress with a commercial power filter. Moreover, the conventional MPDPC strategy implements a single inverter voltage vector during each duty cycle, so serious harmonics will appear in current and power. To improve the steady-state performance of the MPDPC strategy, a high sampling frequency is needed, which is contradictory to its long calculation time due to the iterative calculation process for predictions.

To improve the steady-state operational performance, the two-vector based MPDPC strategies were introduced (Zhang and Zhu, 2011; Zhang et al., 2013, 2014, 2016; Choi and Lee, 2015; Fang et al., 2016). Two voltage vectors work together with suitable duration times calculated by minimizing the cost function. However, the active and reactive power errors cannot be removed simultaneously with only two vectors (Cheng et al., 2017). Moreover, a varying switching frequency is inevitable.

To eliminate the active and reactive power errors at the same time, a novel MPDPC strategy implementing two adjacent active inverter voltage vectors and one zero inverter voltage vector was proposed by Larrinaga et al. (2007). The drive signals were arranged into a symmetrical 3+3 pattern so that a constant switching frequency can be obtained. The three voltage vectors were selected based on the sector where the grid voltage vector is located. Their duration times can be predicted according to the dead-beat principle. However, as pointed out by Hu and Zhu (2013), Hu (2013), and Cheng et al. (2017), the calculated duration times would be negative due to this voltage vector selection method, which could not be implemented in practical applications and thus will deteriorate the system performance.

Hu and Zhu (2013) tried to solve the above problem by reselecting the active inverter voltage vector, which, however, increases the switching frequency and the computational burden on the digital signal processor (DSP). Another approach was proposed by Hu (2013), where the required inverter voltage vector can be calculated by introducing the virtual flux, and the negative duration time can be avoided. However, calculation of the virtual flux involves the integral of grid voltages. The integral initial value may influence the selection of the voltage vectors. Cheng et al. (2017) proposed a novel method with optimized switching patterns based on an automatic updating mechanism, which updates the pre-selected vectors to more suitable ones when the duration times are negative. However, the method is complicated.

It was pointed out by Aguilera et al. (2013) and Vazquez et al. (2015) that there exist both magnitude and phase differences between the grid voltage vector and the required inverter voltage vector when the power flows through the GCI system. So, it may be not precise to select the inverter voltage vectors based on the sector where the grid voltage vector is located. Vazquez et al. (2015) adopted a cost function to evaluate all the possible combinations of adjacent active inverter voltage vectors, and the one that has the minimum cost function value was selected for implementation during the next duty cycle, which is difficult to use in commercial DSPs.

A novel three-vector based dead-beat MPDPC strategy is proposed for the GCI in this paper. The three inverter voltage vectors are selected based on the active and reactive power errors rather than the sector where the grid voltage vector is located, which ensures positive duration times of the selected vectors. Compared with the methods proposed by Hu and Zhu (2013), the proposed one does not need to judge the sign of the predicted duration times, and the corresponding calculation of duration times for the newly selected voltage vectors is avoided. No additional virtual flux as in Hu (2013) is needed. We will first summarize the principles of the one-vector, two-

vector, and conventional three-vector based MPDPC strategies. The drawback of the conventional three-vector based MPDPC due to negative duration times is explained. Then the proposed strategy is discussed in detail. Finally, an experimental setup is constructed and the experimental results are provided.

2 Dead-beat MPDPC strategy

First, the mathematical model of GCI is given for prediction purposes. Then the principles of one-vector, two-vector, and conventional three-vector based MPDPC strategies are briefly described. In the conventional three-vector based MPDPC strategy, the predicted duration times of the active inverter voltage vectors, selected based on the angular position of the grid voltage vector, turn out to be negative in some regions.

2.1 Predictive model of GCI

The schematic of the three-phase GCI is shown in Fig. 1. The mathematical model in the stationary $\alpha\beta$ reference frame can be written as

$$\boldsymbol{u}_{g\alpha\beta}=R_g\boldsymbol{i}_{g\alpha\beta}+L_g\frac{\mathrm{d}\boldsymbol{i}_{g\alpha\beta}}{\mathrm{d}t}+\boldsymbol{v}_{g\alpha\beta}, \tag{1}$$

where $\boldsymbol{u}_{g\alpha\beta}$, $\boldsymbol{i}_{g\alpha\beta}$, and $\boldsymbol{v}_{g\alpha\beta}$ are the grid voltages, currents, and inverter voltages in the $\alpha\beta$ reference frame, respectively, and L_g and R_g are the inductance and parasitic resistances of the grid-connected filter, respectively.

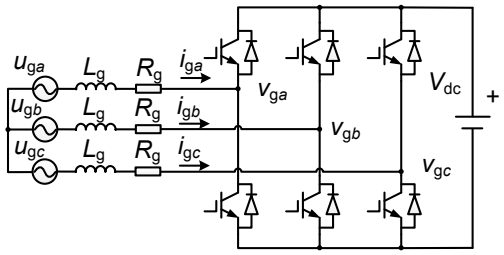

Fig. 1 Schematic of the three-phase grid-connected inverter (GCI)

Based on instantaneous power theory, the apparent power generated into the grid can be written as

$$\boldsymbol{S}=P_g+\mathrm{j}Q_g=-\frac{3}{2}(\hat{\boldsymbol{i}}_{g\alpha\beta}\cdot\boldsymbol{u}_{g\alpha\beta}), \tag{2}$$

where '^' indicates the conjugate value.

The derivative of the apparent power is written as

$$\begin{aligned}\frac{\mathrm{d}\boldsymbol{S}}{\mathrm{d}t}&=-\frac{3}{2}\left(\frac{\mathrm{d}\hat{\boldsymbol{i}}_{g\alpha\beta}}{\mathrm{d}t}\boldsymbol{u}_{g\alpha\beta}+\frac{\mathrm{d}\boldsymbol{u}_{g\alpha\beta}}{\mathrm{d}t}\hat{\boldsymbol{i}}_{g\alpha\beta}\right)\\&=-\frac{3}{2}\left[\boldsymbol{u}_{g\alpha\beta}\frac{1}{L_g}(\hat{\boldsymbol{u}}_{g\alpha\beta}-R_g\hat{\boldsymbol{i}}_{g\alpha\beta}-\hat{\boldsymbol{v}}_{g\alpha\beta})+\mathrm{j}\omega\hat{\boldsymbol{i}}_{g\alpha\beta}\boldsymbol{u}_{g\alpha\beta}\right]\\&=\frac{1}{L_g}\left[-\frac{3}{2}U_g^2+(R_g-\mathrm{j}\omega L_g)\boldsymbol{S}+\frac{3}{2}\boldsymbol{u}_{g\alpha\beta}\hat{\boldsymbol{v}}_{g\alpha\beta}\right],\end{aligned} \tag{3}$$

where U_g is the amplitude of the grid voltage vector and ω is the angular speed of the grid voltage vector.

2.2 One-vector based MPDPC

The MPDPC strategy for the GCI was first proposed by Cortes et al. (2008b). During each duty cycle, future active and reactive powers at the beginning of the next duty cycle can be predicted by evaluating all the possible inverter voltage vectors. Then a cost function is adopted to select the most suitable inverter voltage vector that results in the minimum cost function value. The selected inverter voltage vector will be implemented during the next duty cycle. The delay compensation proposed by Cortes et al. (2008b) is adopted in this study. The detailed predictive algorithm is deduced as follows.

Assume that s_p^k and s_q^k are the gradients of the active and reactive powers at instant t^k for the selected voltage vector calculated during the last duty cycle, which can be calculated based on Eq. (3) as

$$\begin{cases}s_p^k=\dfrac{1}{L_g}\left[-\dfrac{3}{2}(U_g^k)^2+R_gP_g^k+\omega L_gQ_g^k\right.\\\qquad\left.+\dfrac{3}{2}(u_{g,\alpha}^kv_{g,\alpha}^k+u_{g,\beta}^kv_{g,\beta}^k)\right],\\s_q^k=\dfrac{1}{L_g}\left[R_gQ_g^k-\omega L_gP_g^k+\dfrac{3}{2}(u_{g,\beta}^kv_{g,\alpha}^k-u_{g,\alpha}^kv_{g,\beta}^k)\right].\end{cases} \tag{4}$$

The active and reactive power P_g^k and Q_g^k at instant t^k can be calculated using Eq. (2). Then, the active and reactive powers P_g^{k+1} and Q_g^{k+1} at instant t^{k+1}

can be predicted using the first Euler difference equation for delay compensation:

$$\begin{cases} P_{\mathrm{g}}^{k+1} = P_{\mathrm{g}}^{k} + s_p^k T_{\mathrm{s}}, \\ Q_{\mathrm{g}}^{k+1} = Q_{\mathrm{g}}^{k} + s_q^k T_{\mathrm{s}}, \end{cases} \tag{5}$$

where T_{s} is the control period of the duty cycle.

Based on the compensated powers P_{g}^{k+1} and Q_{g}^{k+1}, the iterative prediction process of evaluating all the possible inverter voltage vectors can be implemented to obtain the future powers P_{g}^{k+2} and Q_{g}^{k+2} at instant t^{k+2}:

$$\begin{cases} P_{\mathrm{g}}^{k+2} = P_{\mathrm{g}}^{k+1} + s_p^{k+1} T_{\mathrm{s}}, \\ Q_{\mathrm{g}}^{k+2} = Q_{\mathrm{g}}^{k+1} + s_q^{k+1} T_{\mathrm{s}}. \end{cases} \tag{6}$$

In a three-phase two-level inverter, there exist seven different inverter voltage vectors, and seven different predicted powers of P_{g}^{k+2} and Q_{g}^{k+2} can be obtained. To select the most suitable voltage vector, a cost function defined in Eq. (7) is used:

$$\mathrm{CF} = (P_{\mathrm{g}}^{*,k+2} - P_{\mathrm{g}}^{k+2})^2 + (Q_{\mathrm{g}}^{*,k+2} - Q_{\mathrm{g}}^{k+2})^2. \tag{7}$$

The inverter voltage vector that has the minimum cost function value would be implemented during the next duty cycle so that the real active and reactive powers can always follow their reference values.

As can be seen, the conventional MPDPC strategy employs a single inverter voltage vector during each duty cycle. Thus, large ripples would be generated in the line current and power. Moreover, the iterative prediction process increases the computational burden on the DSP. To improve the steady-state operational performance of GCI, a two-vector based MPDPC strategy has been proposed.

2.3 Two-vector based MPDPC

The two-vector based MPDPC strategy implements two inverter voltage vectors during each duty cycle. Two problems need to be solved for the two-vector based MPDPC strategy: selection of inverter voltage vectors and calculations of their duty times. The first active inverter voltage vector can be selected among the six active inverter voltage vectors in a way similar to that of the one-vector based MPDPC strategy. The second inverter voltage vector could be either the zero inverter voltage vector (Zhang and Zhu, 2011, Zhang et al., 2013, 2014; Choi and Lee, 2015) or the active inverter voltage vector (Fang et al., 2016; Zhang et al., 2016).

The delay compensation is similar to that in the one-vector based MPDPC strategy and will not be repeated here. Assume that at t^{k+1}, s_1 and s_{11} are the active and reactive power gradients when applying the first active vector, s_2 and s_{22} the power gradients when applying the second active vector, which can be calculated as shown in Eq. (4) by replacing k with k+1, and t_1 the duration time that the first vector lasts. The system power at t^{k+2} can be calculated as

$$\begin{cases} P_{\mathrm{g}}^{k+2} = P_{\mathrm{g}}^{k+1} + s_1 t_1 + s_2 (T_{\mathrm{s}} - t_1), \\ Q_{\mathrm{g}}^{k+2} = Q_{\mathrm{g}}^{k+1} + s_{11} t_1 + s_{22} (T_{\mathrm{s}} - t_1). \end{cases} \tag{8}$$

The cost function is still defined as Eq. (7). The minimum value of CF can be obtained if the following condition is satisfied:

$$\frac{\mathrm{dCF}}{\mathrm{d}t_1} = 0. \tag{9}$$

Thus, t_1 can be obtained by solving Eq. (9):

$$t_1 = \frac{(P_{\mathrm{g}}^{*,k+2} - P_{\mathrm{g}}^{k+1})(s_1 - s_2) + (Q_{\mathrm{g}}^{*,k+2} - Q_{\mathrm{g}}^{k+1})(s_{11} - s_{22})}{(s_1 - s_2)^2 + (s_{11} - s_{22})^2} + \frac{T_{\mathrm{s}}(s_2^2 + s_{22}^2 - s_1 s_2 - s_{11} s_{22})}{(s_1 - s_2)^2 + (s_{11} - s_{22})^2}. \tag{10}$$

However, only t_1 can be controlled in the two-vector based MPDPC strategy, but there are two control targets: active and reactive power errors. Thus, there are still power errors in the two-vector based strategy.

2.4 Conventional three-vector based MPDPC

In the conventional three-vector based MPDPC strategy proposed by Larrinaga et al. (2007), the three inverter voltage vectors are selected (Fig. 2). When the grid voltage vector locates in sector I, V_1, V_2, and V_7 are chosen as the active and zero vectors. Table 1 lists the vector selection results in all the six vectors,

where V_{a1} and V_{a2} are the two active vectors and V_{zero} is the zero vector.

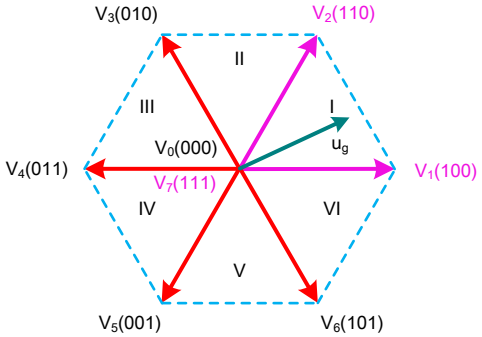

Fig. 2 Sector definition and the inverter voltage vector selection principle

Table 1 Inverter voltage vector selection results when using the conventional dead-beat MPDPC strategy

Sector	V_{a1}	V_{a2}	V_{zero}
I	V_1	V_2	V_7
II	V_3	V_2	V_0
III	V_3	V_4	V_7
IV	V_5	V_4	V_0
V	V_5	V_6	V_7
VI	V_1	V_6	V_0

s_1, s_{11}, s_2, and s_{22} have the same definitions as in the two-vector based MPDPC strategy. Moreover, assume that s_0 and s_{00} are the active and reactive power gradients respectively when applying the zero vector. s_1, s_{11}, s_2, s_{22}, s_0, and s_{00} can also be calculated using Eq. (4) by replacing k with k+1 after delay compensation. t_1 and t_2 are the duration times of V_{a1} and V_{a2}, respectively. Then V_{zero} will last (T_s−t_1−t_2). Thus, the system power at t^{k+2} can be predicted as

$$\begin{cases} P_g^{k+2} = P_g^{k+1} + s_1 t_1 + s_2 t_2 + s_0 (T_s - t_1 - t_2), \\ Q_g^{k+2} = Q_g^{k+1} + s_{11} t_1 + s_{22} t_2 + s_{00} (T_s - t_1 - t_2). \end{cases} \tag{11}$$

To achieve dead-beat control of both active and reactive powers at t^{k+2}, the following condition should be met:

$$\begin{cases} P_g^{k+2} = P_g^{*,k+2}, \\ Q_g^{k+2} = Q_g^{*,k+2}, \end{cases} \tag{12}$$

where $P_g^{*,k+2}$ and $Q_g^{*,k+2}$ are the reference values for active and reactive powers, respectively.

Based on Eq. (12), the duration times t_1 and t_2 can be calculated as

$$\begin{cases} t_1 = [(P_g^{*,k+2} - P_g^{k+1} - s_0 T_s)(s_{22} - s_{00}) \\ \quad - (Q_g^{*,k+2} - Q_g^{k+1} - s_{00} T_s)(s_2 - s_0)] \\ \quad \cdot [(s_1 - s_0)(s_{22} - s_{00}) - (s_{11} - s_{00})(s_2 - s_0)]^{-1}, \\ t_2 = [(P_g^{*,k+2} - P_g^{k+1} - s_0 T_s)(s_{11} - s_{00}) \\ \quad - (Q_g^{*,k+2} - Q_g^{k+1} - s_{00} T_s)(s_1 - s_0)] \\ \quad \cdot [(s_2 - s_0)(s_{11} - s_{00}) - (s_1 - s_0)(s_{22} - s_{00})]^{-1}. \end{cases} \tag{13}$$

Then the selected inverter voltage vectors can be applied during the next duty cycle along with their respective duration times.

2.5 Drawbacks of conventional three-vector based MPDPC

The three-vector MPDPC strategy can greatly improve the steady-state performance of the GCI. The active and reactive power errors can be removed simultaneously in one duty cycle, and the dead-beat control effects can be achieved. However, the duration times of the selected inverter voltage vectors may turn out to be negative in some regions because of an inappropriate method of selecting inverter voltage vectors, as illustrated below.

The voltage equation of the GCI has been given in Eq. (1), which can be rewritten as

$$\boldsymbol{u}_g = \boldsymbol{u}_X + \boldsymbol{v}_g, \tag{14}$$

where $\boldsymbol{u}_X$ represents the voltage drops on the line resistances and inductances. The vectorial representation of the GCI equation model is shown in Fig. 3. It is assumed that the grid currents $\boldsymbol{i}_g$ lags the grid voltage vector $\boldsymbol{u}_g$ by a power factor angle φ. Due to the existence of $\boldsymbol{u}_X$, a phase error δ would be generated between the grid voltage vector $\boldsymbol{u}_g$ and the inverter voltage vector $\boldsymbol{v}_g$.

Take sector I as an example. Although the grid voltage vector $\boldsymbol{u}_g$ lies in sector I, the inverter voltage vector may lie in sector VI due to the phase error δ. Based on the conventional three-vector based MPDPC strategy, V_1, V_2, and V_7 are selected and applied. However, it is impossible to synthesize $\boldsymbol{v}_g$ using the combination of V_1, V_2, and V_7 with all positive

duration times. As illustrated in Fig. 3, the duration time t_2 of V_2 would be negative when using Eq. (13) to remove the power control errors. A negative duration time cannot be applied in a real physical system. Thus, power ripples would be generated using the conventional three-vector MPDPC strategy (Hu and Zhu, 2013; Hu, 2013, Cheng et al., 2017).

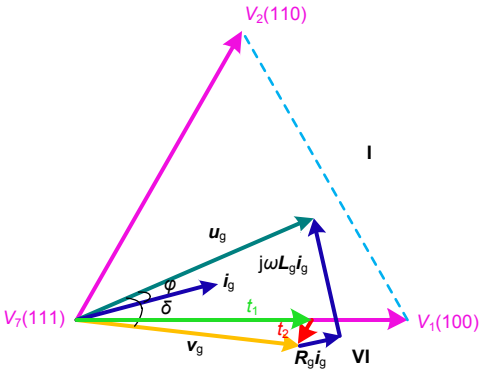

Fig. 3 Vectorial representation of the GCI model to illustrate the reason for a negative predicted duration time in the conventional three-vector based MPDPC strategy

Based on the above analysis, the reason for negative duration times is the inappropriate inverter voltage vector selection method based on the angular position of the grid voltage vector $\boldsymbol{u}_{\mathrm{g}}$. To solve this problem and improve the system performance, a novel three-vector based dead-beat MPDPC method that selects the inverter voltage vectors based on active and reactive power errors will be presented in the following.

3 Improved three-vector based dead-beat MPDPC of the GCI

In this section we will analyze the principle of the proposed MPDPC strategy that adopts a new vector selection method based on the power errors. With the proposed approach, the predicted duration times can be ensured to be always positive and the system performance can be improved.

3.1 Design of the inverter voltage vector selection method

For deduction convenience, Eq. (3) can be rewritten as (Zhang et al., 2013, 2014)

$$\begin{aligned}\frac{\mathrm{d}\hat{\boldsymbol{S}}}{\mathrm{d}t}&=\frac{1}{L_{\mathrm{g}}}\left[-\frac{3}{2}U_{\mathrm{g}}^2+(R_{\mathrm{g}}+\mathrm{j}\omega L_{\mathrm{g}})\hat{\boldsymbol{S}}+\frac{3}{2}\hat{\boldsymbol{u}}_{\mathrm{g}\alpha\beta}\boldsymbol{v}_{\mathrm{g}\alpha\beta}\right]\\&=\frac{1}{L_{\mathrm{g}}}\left[-\frac{3}{2}U_{\mathrm{g}}^2+(R_{\mathrm{g}}+\mathrm{j}\omega L_{\mathrm{g}})\hat{\boldsymbol{S}}+\frac{3}{2}\hat{\boldsymbol{u}}_{\mathrm{g}dq}\boldsymbol{v}_{\mathrm{g}\alpha\beta}\mathrm{e}^{-\mathrm{j}\theta}\right]\\&=\frac{1}{L_{\mathrm{g}}}\left[-\frac{3}{2}U_{\mathrm{g}}^2+(R_{\mathrm{g}}+\mathrm{j}\omega L_{\mathrm{g}})\hat{\boldsymbol{S}}+\frac{3}{2}U_{\mathrm{g}}\boldsymbol{v}_{\mathrm{g}\alpha\beta}\mathrm{e}^{-\mathrm{j}\theta}\right],\end{aligned}\tag{15}$$

where θ is the phase angle of the grid voltage vector, which can be obtained through the phase locked loop (PLL) (Golestan et al., 2017). $\boldsymbol{u}_{\mathrm{g}dq}$ is the grid voltage expressed in the dq synchronous rotating frame, which can be obtained through coordinate transformation with $\boldsymbol{v}_{\mathrm{g}\alpha\beta}$. After delay compensation, the discretization form of Eq. (15) at t^{k+1} can be obtained using the first-order Euler difference equation:

$$\begin{aligned}\hat{\boldsymbol{S}}^{k+2}\mathrm{e}^{\mathrm{j}\theta}=&\left\{\hat{\boldsymbol{S}}^{k+1}+\frac{T_{\mathrm{s}}}{L_{\mathrm{g}}}\left[-\frac{3}{2}(U_g^{k+1})^2\right.\right.\\&\left.\left.+(R_{\mathrm{g}}+\mathrm{j}\omega L_{\mathrm{g}})\hat{\boldsymbol{S}}^{k+1}\right]\right\}\mathrm{e}^{\mathrm{j}\theta}+\frac{3T_{\mathrm{s}}}{2L_{\mathrm{g}}}U_{\mathrm{g}}^{k+1}\boldsymbol{v}_{\mathrm{g}\alpha\beta}^{k+1}.\end{aligned}\tag{16}$$

Let $\Delta\hat{\boldsymbol{S}}^{k+2}$ be the difference between $\hat{\boldsymbol{S}}^{*,k+2}$ and the predicted power $\hat{\boldsymbol{S}}^{k+2}$ at instant t^{k+2}, which can be deduced as

$$\begin{aligned}\Delta\hat{\boldsymbol{S}}^{k+2}\mathrm{e}^{\mathrm{j}\theta}&=[\hat{\boldsymbol{S}}^{*,k+2}-\hat{\boldsymbol{S}}^{k+2}]\mathrm{e}^{\mathrm{j}\theta}\\&=[\hat{\boldsymbol{S}}^{*,k+2}-\hat{\boldsymbol{S}}_0^{k+2}]\mathrm{e}^{\mathrm{j}\theta}-\frac{3T_{\mathrm{s}}}{2L_{\mathrm{g}}}U_{\mathrm{g}}^{k+1}\boldsymbol{v}_{\mathrm{g}\alpha\beta}^{k+1}\\&=\Delta\hat{\boldsymbol{S}}_0^{k+2}\mathrm{e}^{\mathrm{j}\theta}-\frac{3T_{\mathrm{s}}}{2L_{\mathrm{g}}}U_{\mathrm{g}}^{k+1}\boldsymbol{v}_{\mathrm{g}\alpha\beta}^{k+1},\end{aligned}\tag{17}$$

where $\Delta\hat{\boldsymbol{S}}_0^{k+2}$ is the error between $\hat{\boldsymbol{S}}^{*,k+2}$ and $\hat{\boldsymbol{S}}_0^{k+2}$, and $\hat{\boldsymbol{S}}_0^{k+2}$ is the predicted power when only the zero voltage vector works:

$$\hat{\boldsymbol{S}}_0^{k+2}=\hat{\boldsymbol{S}}^{k+1}+\frac{T_{\mathrm{s}}}{L_{\mathrm{g}}}\left[-\frac{3}{2}(U_{\mathrm{g}}^{k+1})^2+(R_{\mathrm{g}}+\mathrm{j}\omega L_{\mathrm{g}})\hat{\boldsymbol{S}}^{k+1}\right].\tag{18}$$

It can be seen from Eq. (17) that dead-beat control of both active and reactive powers can be

obtained if $\Delta\hat{\boldsymbol{S}}^{k+2}$ equals zero, which means that an appropriate equivalent inverter voltage vector $\boldsymbol{v}_{g\alpha\beta}^{k+1}$ needs to be implemented to counteract $\Delta\hat{\boldsymbol{S}}_0^{k+2}e^{j\theta}$. As a result, the three inverter voltage vectors can be selected based on the position of $\Delta\hat{\boldsymbol{S}}_0^{k+2}e^{j\theta}$. In fact, as can be seen in Eq. (17) by setting $\Delta\hat{\boldsymbol{S}}^{k+2}$ to zero, the position of $\Delta\hat{\boldsymbol{S}}_0^{k+2}e^{j\theta}$ is the same as the position of the required $\boldsymbol{v}_{g\alpha\beta}^{k+1}$. After selecting the three inverter voltage vectors, their duration times can also be calculated using the conventional three-vector based MPDPC strategy, as given in Eq. (13).

As shown in Fig. 4, when $\Delta\hat{\boldsymbol{S}}_0^{k+2}e^{j\theta}$ locates at sector I, V_1 and V_2 are selected as the active voltage vectors and V_7 is selected as the zero voltage vector. Note that any vector that lies within sector I can be represented by a linear combination of V_1, V_2, and V_7:

$$\Delta\hat{\boldsymbol{S}}^{k+2}e^{j\theta}=k_1\boldsymbol{V}_1+k_2\boldsymbol{V}_2, \tag{19}$$

where

$$\begin{cases} k_1=\dfrac{3t_1}{2L_g}U_g^{k+1}, \\ k_2=\dfrac{3t_2}{2L_g}U_g^{k+1}. \end{cases} \tag{20}$$

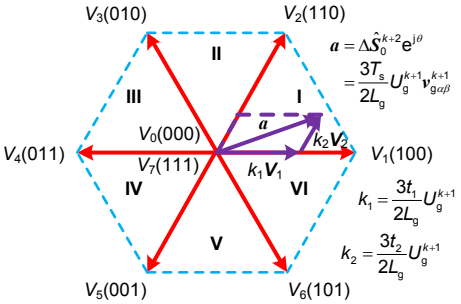

Fig. 4 Selecting inverter voltage vectors based on the position of $\Delta\hat{\boldsymbol{S}}_0^{k+2}e^{j\theta}$

Fig. 4 shows that both k_1 and k_2 are positive. Then t_1 and t_2 are positive according to Eq. (20). Thus, the proposed inverter voltage vector selection method for three-vector based MPDPC can ensure a positive predicted duration time all the time. The voltage vector selection results in other sectors can be referenced in Table 1.

3.2 Drive signal generation

Like the conventional three-vector based MPDPC strategy (Larrinaga et al., 2007), the drive signals are arranged into a symmetrical 3+3 pattern. The whole duty cycle is divided equally into two parts. Drive signals in the two parts are symmetrical in sector I (Fig. 5). The last inverter voltage vector in the first half is the same as the first inverter voltage vector in the second half, and the switching losses can be decreased. Moreover, a constant switching frequency can be obtained, and this is beneficial to the design of ac side filters.

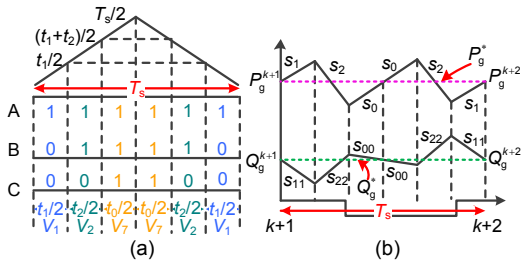

Fig. 5 Symmetrical 3+3 pulse patterns of the three-vector based MPDPC strategy (sector I): (a) pulse patterns in sector I; (b) power variations

Fig. 6 shows the control diagram of the improved three-vector based dead-beat MPDPC strategy. Grid voltages $\boldsymbol{u}_{gabc}^k$ and currents $\boldsymbol{i}_{gabc}^k$ are sampled by voltage and current transducers respectively, based on which the apparent power $\boldsymbol{S}^k$ at instant t^k can be calculated. PLL is adopted to obtain the phase angle θ of the grid voltage vector. After predicting the active

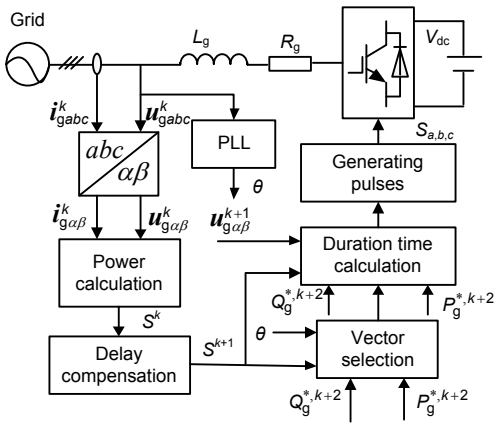

Fig. 6 The control diagram of the improved three-vector based dead-beat MPDPC strategy

power P_g^{k+1} and reactive power Q_g^{k+1} at t^{k+1}, the control delay can be compensated. Based on power errors between the reference values ($P_g^{*,k+2}$ and $Q_g^{*,k+2}$) and the predicted power values $\boldsymbol{S}^{k+1}$, two adjacent active inverter voltage vectors and one zero voltage vector can be selected from Table 1, whose duration times can be calculated using Eq. (13). Drive signals can be generated and arranged into symmetrical 3+3 patterns to control the on and off states of insulated gate bipolar transistors (IGBTs). Thus, the dead-beat control of both active and reactive powers can be realized.

4 Experimental validation

Fig. 7 shows the 1 kW GCI experiment platform. The control algorithm is executed in TMS320F2812. The DC-link voltage is 280 V, which can be obtained from a dc power supply. Three line inductors are used to filter the line currents with the inductance value of 6 mH. The voltage and current transducers are used to obtain the grid voltages and currents. Then DSP executes the conventional or improved MPDPC strategies, and outputs the pulse width modulation (PWM) signals. A Semikron IGBT driver circuit (SKHI 61 R) is used to generate the drive signals for the IGBTs based on the PWM signals from the DSP. The sampling frequency is 10 kHz. A YOKOGAWA DL750 oscilloscope is used to acquire the experimental waveforms. Detailed parameters of the experimental system are listed in Table 2.

4.1 Steady-state performance

Fig. 8 compares the steady-state performances of the conventional and improved three-vector based MPDPC strategies. The active power generated into the power grid is set to 1000 W and the reactive power to 0 var. Both the conventional and improved three-vector based MPDPC strategies show excellent steady-state performance. However, at the end of every sector, the predicted duration times of the selected active inverter voltage vectors turn out to be negative when using the conventional MPDPC strategy (Fig. 9a). The reason for the negative duration time has been analyzed in Section 2. Because of the negative duration time, active power ripples of ±23 W and reactive power ripples of ±45 var are generated (Table 3). Moreover, the grid currents contain ripples when negative duration times appear.

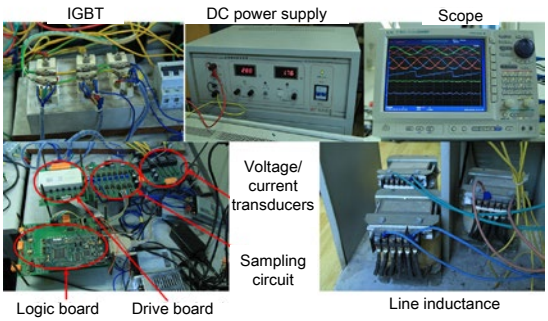

Fig. 7 The 1 kW GCI experiment platform

Table 2 Parameters of the 1 kW GCI system

Parameter	Value
Grid voltage*	156 V
Rated power	1 kW
Rated frequency	50 Hz
Line inductance	6 mH
DC link voltage	280 V
Sampling frequency	10 kHz

* RMS of phase-to-phase voltage

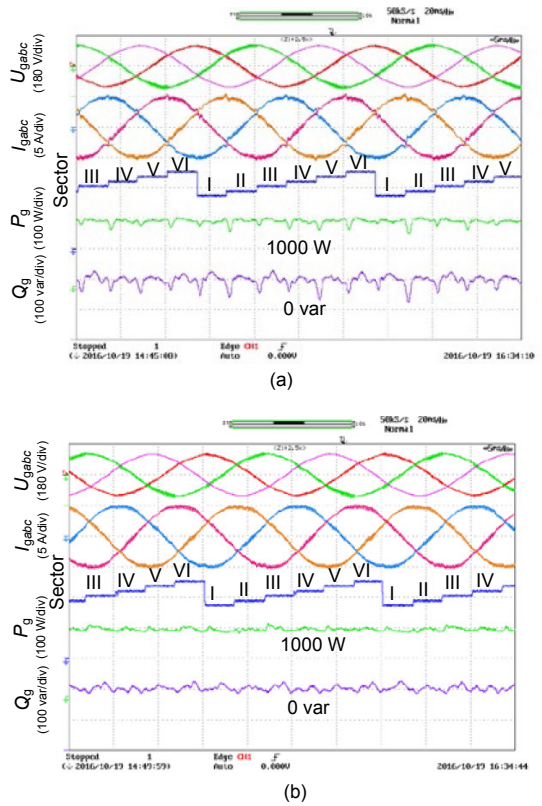

Fig. 8 Comparisons between steady-state responses of the conventional and proposed three-vector based MPDPC strategies with active power equal to 1000 W and reactive power equal to 0 var: (a) conventional three-vector based MPDPC strategy; (b) improved three-vector based MPDPC strategy

Table 3 Power fluctuations and execution times of different MPDPC strategies

Parameter	Value	
	Conventional MPDPC	Improved MPDPC
Fluctuation of P_g (W)	±23	±11
Fluctuation of Q_g (var)	±45	±15
Execution time (μs)	38.5	41.2
THD of currents	5.61%	5.00%

Fig. 8b shows the steady-state performance of the improved three-vector based MPDPC strategy, where the three inverter voltage vectors are selected based on the power errors instead of the angular position of the grid voltage vector. The active and reactive power ripples can be removed and the steady-state performance can be further improved with the active and reactive power fluctuations decreased to ±11 W and ±15 var, respectively (Table 3). The selected active vectors' duration times are positive all the time (Fig. 9b). The grid current curves become smoother using the improved three-vector based MPDPC strategy as the power ripples are removed.

Fig. 10 shows the fast Fourier transform (FFT) analysis results of grid currents using the conventional and improved three-vector based MPDPC strategies. The total harmonic distortion (THD) of the grid currents using the conventional three-vector based MPDPC is 5.61%. The improved three-vector based MPDPC strategy has better grid current qualities of 5.00% THD since the current glitches are removed. Detailed results of FFT analysis of the currents obtained using the conventional and improved MPDPC strategies are listed in Table 4. The amplitudes of harmonic order currents in the improved MPDPC strategy are smaller than those in the conventional MPDPC strategy in most cases. Moreover, both the conventional and improved three-vector based MPDPC strategies lead to a constant switching frequency with the harmonic current components concentrating at around 10 kHz. This would simplify the design process of ac side filters.

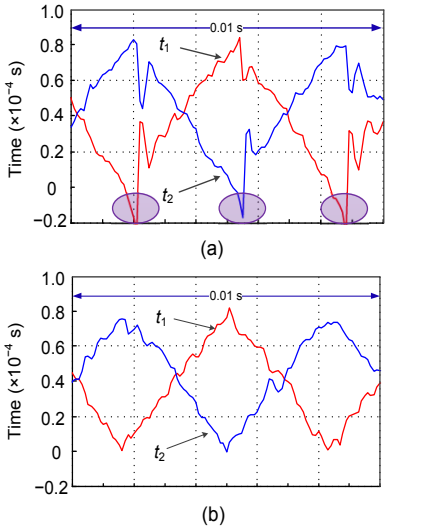

Fig. 9 Predicted duration times of the selected active inverter voltage vectors using the conventional three-vector based MPDPC strategy (a) and the improved three-vector based MPDPC strategy (b)

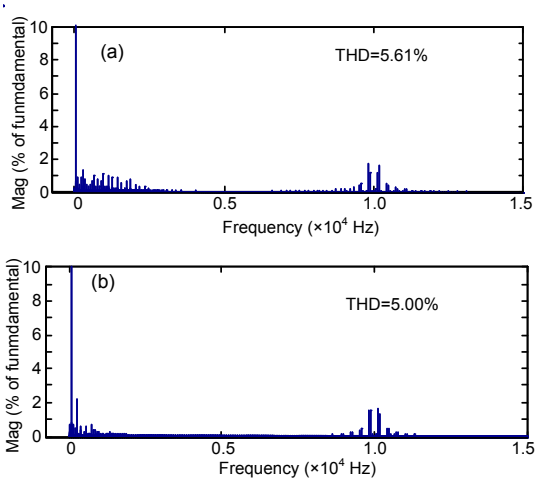

Fig. 10 Current harmonic analysis: (a) conventional three-vector based MPDPC strategy; (b) improved three-vector based MPDPC strategy

Table 3 also gives the execution times of different MPDPC strategies in DSP. The conventional three-vector based MPDPC strategy needs 38.5 μs to run the whole interrupt routine. The improved three-vector based MPDPC strategy needs a little longer execution time of 41.2 μs since additional inverter voltage vector selection algorithms based on power errors are needed.

4.2 Dynamic responses

Fig. 11 gives the dynamic responses of different MPDPC strategies when the active power steps from 500 to 1000 W while the reactive power remains at 0 var. Fig. 12 shows the dynamic responses of the different MPDPC strategies when the reactive power steps from 0 to 500 var while the active power remains at 500 W. The dynamic responses of both

strategies are given within 2 ms when either active or reactive power changes, which is the most outstanding feature of predictive control. The experiment verifies that the improved three-vector based MPDPC strategy still has the merit of fast dynamic response. Moreover, the active and reactive powers are well decoupled. The change of the active power will not influence the reactive power, and vice versa.

Table 4 Comparison of current harmonics between the two MPDPC strategies

Harmonic order	THD in the current		Harmonic order	THD in the current	
	Conventional MPDPC	Improved MPDPC		Conventional MPDPC	Improved MPDPC
2	0.92%	0.68%	12	0.12%	0.10%
3	0.45%	0.41%	13	0.98%	0.21%
4	0.88%	0.49%	14	0.29%	0.15%
5	1.37%	1.22%	15	0.78%	0.72%
6	0.32%	0.12%	16	0.30%	0.40%
7	0.78%	0.38%	17	0.67%	0.36%
8	0.44%	0.55%	18	0.07%	0.20%
9	0.30%	0.10%	19	1.13%	0.25%
10	0.47%	0.31%	20	0.31%	0.12%
11	0.63%	0.56%	21	0.18%	0.16%

THD: total harmonic distortion

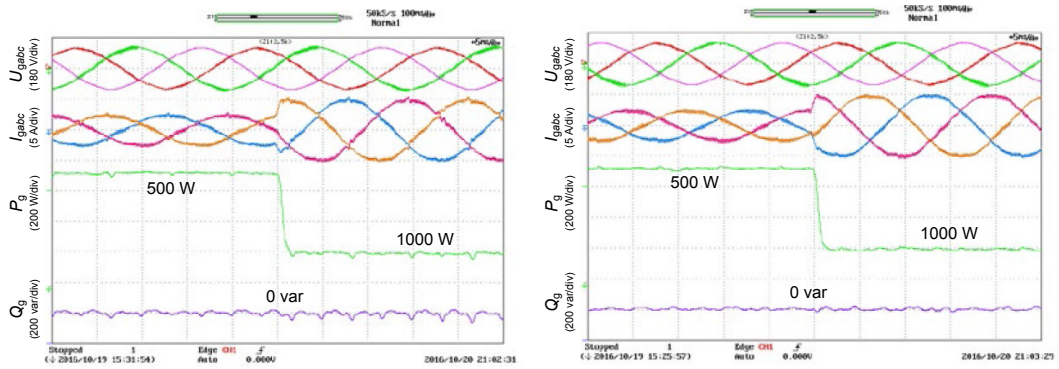

Fig. 11 Comparisons between dynamic responses of different MPDPC strategies with active power stepping from 500 to 1000 W while reactive power kept constant at 0 var: (a) conventional three-vector based MPDPC strategy; (b) improved three-vector based MPDPC strategy

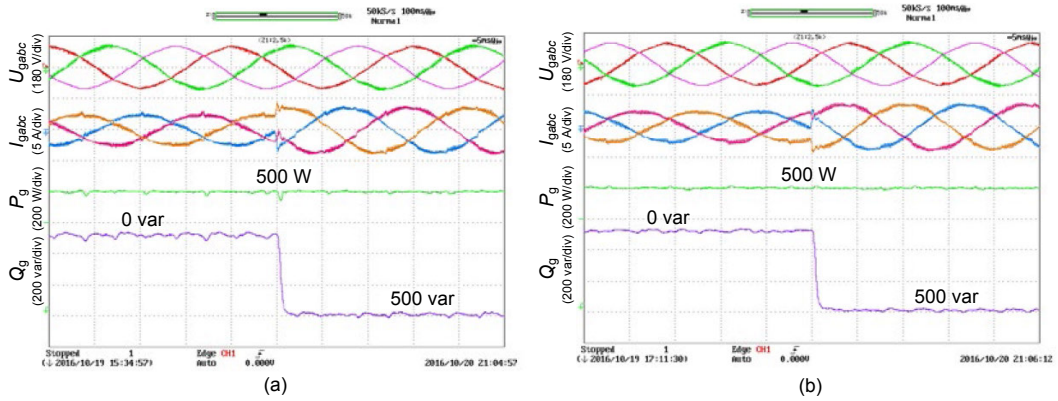

Fig. 12 Comparisons between dynamic responses of different MPDPC strategy with reactive power stepping from 0 to 500 var while active power kept constant at 500 W: (a) conventional three-vector based MPDPC strategy; (b) improved three-vector based MPDPC strategy

5 Conclusions

In this paper we present an improved three-vector based dead-beat MPDPC strategy for the three-phase GCI. Unlike the conventional three-vector MPDPC strategy, the proposed one selects the inverter voltage vectors based on power errors rather than the grid voltage vector position. Thus, the predicted duration times can be ensured to be positive. The proposed three-vector dead-beat MPDPC strategy has the following advantages:

1. Two adjacent active inverter voltage vectors plus one zero inverter voltage vector are applied during every duty cycle, so the switching frequency is kept constant, which simplifies the design process of ac side filters.

2. The proposed method of selecting the inverter voltage vectors based on active and reactive power errors can eliminate power ripples and further improve the steady-state performance.

3. The iterative computation process in the conventional predictive control strategy is avoided. Thus, the execution time can be decreased, and less calculation capacity of the DSP is demanded.

4. Dynamic responses of the improved three-vector based dead-beat MPDPC strategy are still fast.

References

Aguilera RP, Quevedo DE, Vazquez S, et al., 2013. Generalized predictive direct power control for AC/DC converters. Proc IEEE ECCE Asia Downunder, p.1215-1220. https://doi.org/10.1109/ECCE-Asia.2013.6579263

Blasko V, Kaura V, 1997. A new mathematical model and control of a three-phase AC-DC voltage source converter. *IEEE Trans Power Electron*, 12(1):116-123. https:// doi.org/10.1109/63.554176

Chen X, Zhang Y, Wang SS, et al., 2017. Impedance-phased dynamic control method for grid-connected inverters in a weak grid. *IEEE Trans Power Electron*, 32(1):274-283. https://doi.org/10.1109/TPEL.2016.2533563

Cheng CW, Nian H, Wang XH, et al., 2017. Dead-beat predictive direct power control of voltage source inverters with optimized switching patterns. *IET Power Electron*, 10(12):1438-1451. https://doi.org/10.1049/iet-pel.2016.0869

Choi DK, Lee KB, 2015. Dynamic performance improvement of AC/DC converter using model predictive direct power control with finite control set. *IEEE Trans Ind Electron*, 62(2):757-767. https://doi.org/10.1109/TIE.2014.2352214

Cortes P, Rodriguez J, Quevedo DE, et al., 2008a. Predictive current control strategy with imposed load current spectrum. *IEEE Trans Power Electron*, 23(2):612-618. https://doi.org/10.1109/TPEL.2007.915605

Cortes P, Rodriguez J, Antoniewicz P, et al., 2008b. Direct power control of an AFE using predictive control. *IEEE Trans Power Electron*, 23(5):2516-2523. https://doi.org/10.1109/TPEL.2008.2002065

Dekka A, Wu B, Yaramasu V, et al., 2017. Model predictive control with common-mode voltage injection for modular multilevel converter. *IEEE Trans Power Electron*, 32(3): 1767-1778. https://doi.org/10.1109/TPEL.2016.2558579

Fang H, Zhang ZB, Feng XY, et al., 2016. Ripple-reduced model predictive direct power control for active front-end power converters with extended switching vectors and time-optimised control. *IET Power Electron*, 9(9):1914-1923. https://doi.org/10.1049/iet-pel.2015.0857

Golestan S, Guerrero JR, Vasquez JC, 2017. Three-phase PLLs: a review of recent advances. *IEEE Trans Power Electron*, 32(3):1894-1907. http://dx.doi.org/10.1109/TPEL.2016.2565642

Hu JB, 2013. Improved dead-beat predictive DPC strategy of grid-connected dc-ac converters with switching loss minimization and delay compensations. *IEEE Trans Ind Inform*, 9(2):728-738. https://doi.org/10.1109/TII.2012.2223705

Hu JB, Zhu ZQ, 2013. Improved voltage-vector sequences on dead-beat predictive direct power control of reversible three-phase grid-connected voltage-source converters. *IEEE Trans Power Electron*, 28(1):254-267. https://doi.org/10.1109/TPEL.2012.2194512

Larrinaga SA, Vidal MAR, Oyarbide E, et al., 2007. Predictive control strategy for DC/AC converters based on direct power control. *IEEE Trans Ind Electron*, 54(3):1261-1271. https://doi.org/10.1109/TIE.2007.893162

Malinowiski M, 2001. Sensorless control strategies for three-phase PWM rectifiers. PhD Thesis, Warsaw University of Technology, Warsaw, Poland.

Rodriguez JR, Dixon JW, Espinoza JR, et al., 2005. PWM regenerative rectifiers: state of the art. *IEEE Trans Ind Electron*, 52(1):5-22. https://doi.org/10.1109/TIE.2004.841149

Song ZF, Chen W, Xia CL, 2014. Predictive direct power control for three-phase grid-connected converters without sector information and voltage vector selection. *IEEE Trans Power Electron*, 29(10):5518-5531. https://doi.org/10.1109/TPEL.2013.2289982

Vargas R, Cortes P, Ammann U, et al., 2007. Predictive control of a three-phase neutral-point-clamped inverter. *IEEE Trans Ind Electron*, 54(5):2697-2705. https://doi.org/10.1109/TIE.2007.899854

Vazquez S, Marquez A, Aguilera R, et al., 2015. Predictive optimal switching sequence direct power control for grid-connected power converters. *IEEE Trans Ind Electron*, 62(4):2010-2020. https://doi.org/10.1109/TIE.2014.2351378

Zeng Z, Li H, Tang SQ, et al., 2016. Multi-objective control of multi-functional grid-connected inverter for renewable energy integration and power quality service. *IET Power Electron*, 9(4):761-770. https://doi.org/10.1049/iet-pel.2015.0317

Zhang YC, Zhu JG, 2011. A novel duty cycle control strategy to reduce both torque and flux ripples for DTC of permanent magnet synchronous motor drives with switching frequency reduction. *IEEE Trans Power Electron*, 26(10): 3055-3067. https://doi.org/10.1109/TPEL.2011.2129577

Zhang YC, Xie W, Li ZX, et al., 2013. Model predictive direct power control of a PWM rectifier with duty cycle optimization. *IEEE Trans Power Electron*, 28(11):5343-5351. https://doi.org/10.1109/TPEL.2013.2243846

Zhang YC, Xie W, Li ZX, et al., 2014. Low-complexity model predictive power control: double-vector-based approach. *IEEE Trans Ind Electron*, 61(11):5871-5880. https://doi.org/10.1109/TIE.2014.2304935

Zhang YC, Peng YB, Yang HT, 2016. Performance improvement of two-vector-based model predictive control of PWM rectifier. *IEEE Trans Power Electron*, 31(8): 6016-6030. https://doi.org/10.1109/TPEL.2015.2498306

Zhao QS, Ye YQ, Xu GF, et al., 2016. Improved repetitive control scheme for grid-connected inverter with frequency adaptation. *IET Power Electron*, 9(5):883-890. https://doi.org/10.1049/iet-pel.2015.0057